Available online at www.sciencedirect.com
ScienceDirect
Journal of the European Ceramic Society 27 (2007) 475–478
www.elsevier.com/locate/jeurceramsoc

Thermal conductivity of pressed powder compacts: tin oxide and alumina

C. Poulier, D.S. Smith *, J. Absi

Groupe d'Étude des Matériaux Hétérogènes, École Nationale Supérieure de Céramique Industrielle, 47-73 Avenue Albert Thomas, 87 065 Limoges Cedex, France

Available online 5 June 2006

Abstract

Three aspects, which significantly reduce heat transfer through a polycrystalline material, are considered in this paper: porosity, grain boundary thermal resistance and the state of the grain–grain contacts. Tin oxide and alumina were chosen as model systems. Tin oxide, without a sintering additive, does not densify during thermal treatment but grain growth is not inhibited and consequently the microstructure can be varied. In alumina, variation of the thermal treatment conditions varies both grain size and porosity. Thermal conductivity measurements, using the laser-flash technique, reveal that the thermal resistance of a pressed powder compact is almost independent of temperature and at least a factor of 2.5 greater than a consolidated material with similar pore volume fraction and grain size. The reduced contact area of the grain–grain interfaces in the green body can explain this as demonstrated by numerical simulation. We also show that larger grain size increases the thermal conductivity of the porous ceramic.

Keywords: Sintering; Grain boundaries; Porosity; Thermal conductivity; Tin oxide

1. Introduction

A large amount of experimental data on the thermal properties of dense and porous ceramics can be found in the literature. This is relevant to the performance of the ceramic material in working conditions. The thermo-physical characteristics also play an important role for the response of the ceramic body to the conditions during the fabrication process. For example, the question can be asked whether a homogeneous temperature is achieved rapidly during the firing cycle. This is determined in part by the heat capacity and the thermal conductivity of the solid. However, the ceramic material exhibits strongly different microstructures before and after firing. The thermo-physical characteristics will also evolve significantly. We have chosen to study in particular the evolution of the thermal conductivity of a material from the pressed powder compact (green body) to the final sintered ceramic.

In a porous polycrystalline dielectric solid, subjected to a thermal gradient, the major part of the heat is carried by vibrations in the solid skeleton. Generally the presence of obstacles such as pores and grain boundaries decreases significantly the heat flow and hence the effective thermal conductivity of the material. These aspects are examined in terms of thermal response at the microscopic scale using numerical simulation.

The essential transformations of the microstructure during firing involve the nature of the grain–grain contacts (cohesion of powder compact), elimination of porosity and grain growth. The influence of these factors on the variation of the equivalent thermal conductivity has been studied by comparison of experimental measurements for green bodies to samples with thermal treatments which progressively go to higher temperatures. Two materials were chosen for investigation, tin oxide and alumina. Pure tin oxide presents a rather particular advantage. There is virtually no change in the pore volume fraction between the green body and the "sintered" compacts. In contrast the grain size increases significantly for thermal treatments of 1300 °C and above. This means a set of microstructures could be prepared where one of the microstructural variables (porosity) has been fixed at a constant value. Alumina is an economically important ceramic oxide which has an intrinsic thermal conductivity ($35\,W\,m^{-1}\,K^{-1}$) close to tin oxide ($40\,W\,m^{-1}\,K^{-1}$). However, the microstructural evolution during firing is more complex with porosity elimination as well. We just present some preliminary results for the thermal conductivity of the green body between

* Corresponding author. Tel.: +33 5 55 45 22 30; fax: +33 5 55 79 09 98.
E-mail address: d_smith@ensci.fr (D.S. Smith).

0955-2219/$ – see front matter © 2006 Elsevier Ltd. All rights reserved.
doi:10.1016/j.jeurceramsoc.2006.04.068

room temperature and 400 °C for comparison to the tin oxide samples. For convenience the results of the numerical models (first part) and the experimental measurements (second part) have been presented in terms of thermal resistivity (λ^{-1}) rather than conductivity (λ).

2. Experimental

2.1. Sample preparation

Tin oxide samples were prepared from a commercial high purity powder (Aldrich), previously heated for 4 h at 400 °C. Samples were uniaxially pressed at 125 MPa without any binder into cylinders 2 mm thick and 13 mm in diameter. Some of these were sintered at various temperature dwells from 1000 °C to 1500 °C for 0.2 h after a heating ramp of 60 °C/min. In the same way, alumina green bodies were prepared from a commercial powder P172SB (Pechiney). Both powders have a specific surface area of approximately 10 $m^2\,g^{-1}$. The average grain size was 0.3 μm for the alumina powder and 0.1 μm for the tin oxide powder.

2.2. Characterization

The thermal conductivity λ was evaluated using the laser-flash method. This transient technique consists of heating the front face of the sample by an optical pulse of duration 450 μs delivered by a neodymium glass laser. The temperature–time behaviour of the rear face is monitored by an infrared detector. The signal is then sent to a preamplifier and recorded by a numerical oscilloscope. The temperature–time behaviour is analysed to determine characteristic times necessary for the calculation of thermal diffusivity (α) by the equations of Degiovanni which take heat losses into account. The thermal conductivity (λ) was then calculated from the expression:

$$\lambda = \alpha \cdot \rho \cdot c \tag{1}$$

where ρ is the sample density and c is the specific heat.

Specific heat values were taken from literature. The pore volume fraction was evaluated by measurement of the sample density using the method based on Archimedes' principle. For the green body, an evaluation is made using geometrical dimensions and mass. The average grain size was evaluated using the linear intercept method. This varied from 0.2 μm to 4.9 μm for tin oxide samples depending on the sintering dwell temperature.

3. Numerical models: microscopic scale

Numerical simulations were performed with a finite element analysis package, Abaqus. A difference of temperature (ΔT) is applied across the model system until thermal equilibrium is achieved. Then the effective conductivity is obtained from the calculated average heat flow density (Φ) using Fourier's equation:

$$\lambda = \frac{\Phi \cdot e}{\Delta T} \tag{2}$$

where e is the thickness crossed by the heat flow.

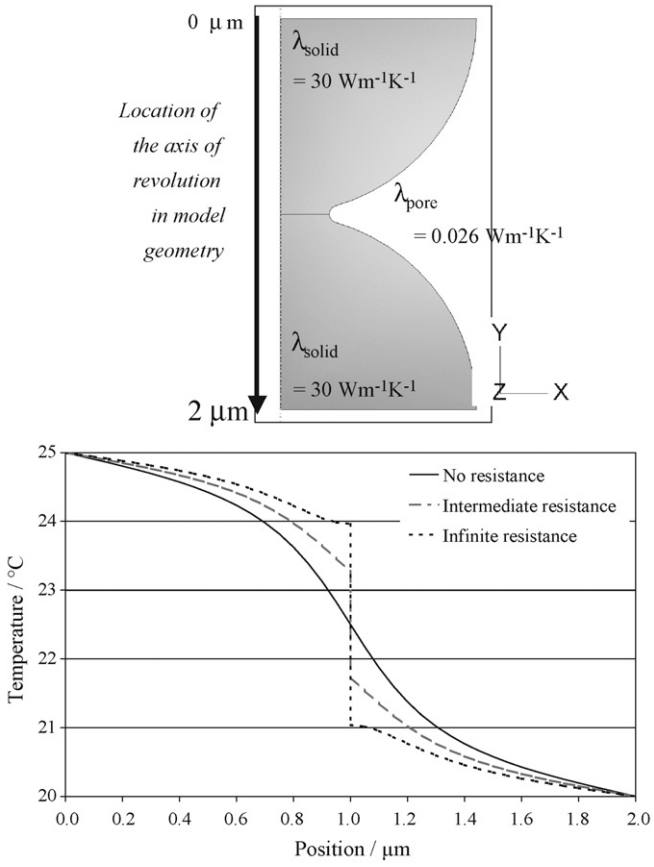

Fig. 1. (Top) Two spheres in contact (Coble geometry) with a grain boundary. (Bottom) Temperature distributions along the axis of revolution for different values of the interface resistance; the intermediate one is $1.0 \times 10^{-8}\ m^2\ KW^{-1}$.

This method was applied to a model of two spheres in contact (Coble geometry,[1] Fig. 1(top)) in order to calculate the resulting temperature distribution along the central axis with and without a grain boundary resistance (Fig. 1(bottom)). On the curve "No resistance", the effect of the constriction on the heat flow is revealed by the increase in the thermal gradient in the vicinity of the neck. With a grain boundary thermal resistance of $1 \times 10^{-8}\ m^2\ KW^{-1}$, corresponding to the literature values for dense polycrystalline ceramics, this becomes a sharp temperature drop at the interface. The influence of grain size variation was studied by changing the length of the axis of revolution with the values: 2 μm, 20 μm, 2 mm and 20 mm. It can be noted that for a perfect contact, despite the constriction, there is no effect on the value of effective thermal conductivity. In contrast the imperfect contact ($1 \times 10^{-8}\ m^2\ KW^{-1}$) yields a decrease in effective thermal conductivity for smaller grain sizes.

To study the role of surface contact area, a simpler geometry was then used. For a two dimensional geometry, two blocks of solid are placed in contact with a variable contact length from 1 mm to 0.2 mm (Fig. 2). There is no porosity incorporated in the system. A temperature difference of 5 °C is applied and the thermal conductivity, given by Fourier's law, is calculated with the value of average heat flow density on the bottom face.

Constriction of the heat flow at the interface gives an increase of thermal resistivity. This effect becomes even stronger when

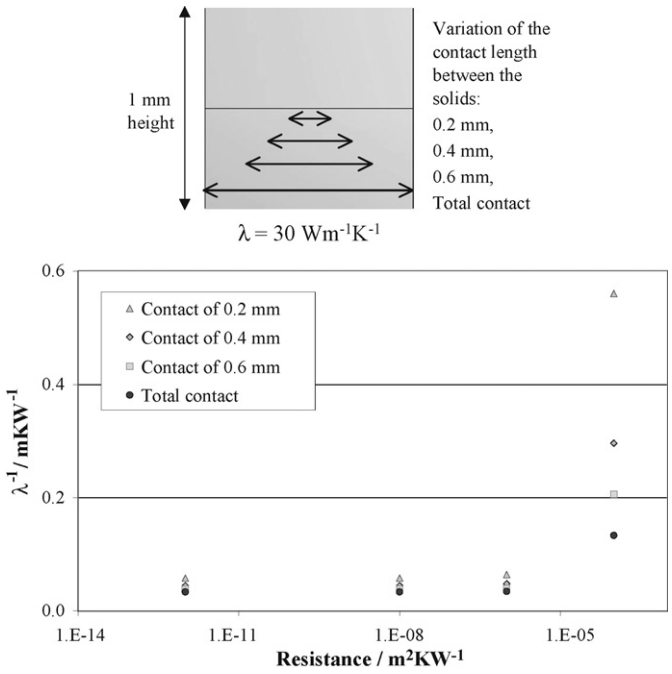

Fig. 2. (Top) Model of two blocks in contact; no porosity is introduced; the contact length is variable from 0.2 mm to 1 mm (total contact). (Bottom) Resistivity as a function of interface resistance for the four models.

the thermal resistance at the interface is relatively significant compared to the thermal resistance of the blocks.

Now, porosity is introduced. Increase of porosity corresponds to a decrease of the contact surface area (Fig. 3), and has a non-negligible effect on the effective thermal resistivity. For example, the value is increased by a factor of 3 between 16% and 48% porosity. The effect of the thermal resistance at the interface is to increase the overall resistivity of the system.

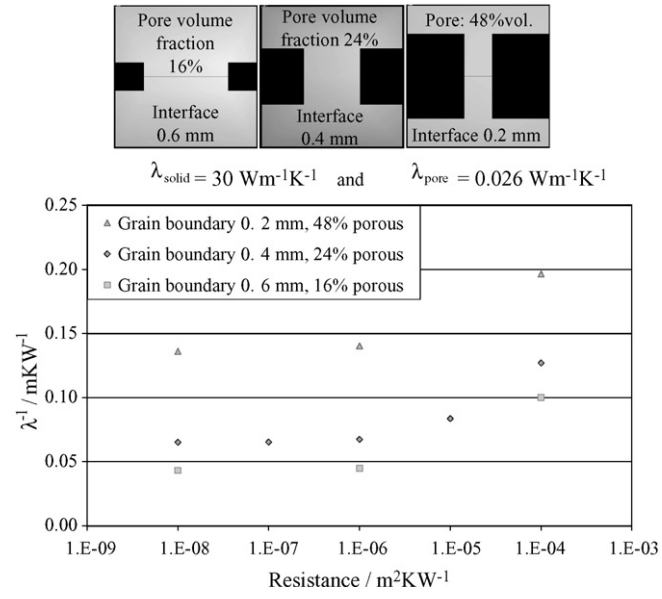

Fig. 3. (Top) Three models where porosity and contact area between the blocks of solid vary strongly. (Bottom) Resistivity variation as a function of interface resistance for the three models.

4. Results

Experimental measurements of the thermal conductivity from room temperature to 400 °C were made for tin oxide and alumina green bodies and also tin oxide samples fired above 1000 °C. Because the geometrical fluctuations of the microstructures are at the micrometer scale the values correspond to the effective thermal conductivity of a homogeneous medium at the macroscopic scale.

4.1. Influence of grain boundary and pores

The following approach can be used to describe the effective thermal conductivity of a porous polycrystalline dielectric solid. A thermal resistance is associated with each grain and grain boundary in the heat path. Using a similar approach to ac impedance studies of ceramics (the brick layer model), the thermal conductivity of the dense polycrystalline material λ_s is given by a simple series model:

$$\frac{1}{\lambda_s} = \frac{1}{\lambda_{crystal}} + n \cdot R_{int} \tag{3}$$

where $\lambda_{crystal}$ is the single crystal thermal conductivity, n the number of grain boundaries per unit length of heat path and R_{int} is the grain boundary thermal resistance per unit area. In earlier work we have used this relation to obtain average values for the grain boundary thermal resistance by fabrication of sets of dense ceramics with variable grain size. The grain boundary thermal resistance was evaluated at 1.0×10^{-8} m^2 KW^{-1} in alumina and 1.2×10^{-8} m^2 KW^{-1} in tin oxide.[2] It can be noted that the first term of Eq. (3) should follow approximately linear behaviour with temperature due to predominance of phonon–phonon scattering in the polycrystalline material.

For materials containing randomly dispersed pores, Landauer's effective medium expression[3] can be used to describe the thermal conductivity of this two-phase system. This is given by:

$$\lambda = \frac{1}{4}[\lambda_p(3v_p - 1) + \lambda_s(2 - 3v_p) + \{[\lambda_p(3v_p - 1) + \lambda_s(2 - 3v_p)]^2 + 8\lambda_s\lambda_p\}^{1/2}] \tag{4}$$

where λ_s is the solid phase thermal conductivity, λ_p the thermal conductivity of the pore phase and v_p is the pore volume fraction.

4.2. Experimental results

The five samples of SnO_2 in Fig. 4 have approximately the same pore volume fraction ($v_p = 0.47$). It can be seen that the thermal resistivity decreases with the increase of grain size. This behaviour is well described by Eq. (3) where the contribution of the grain boundary term becomes progressively smaller as n decreases. The predominance of the grain boundary resistance in the small grain samples (0.2 μm) is also supported by the almost constant value of λ^{-1} with temperature. Theoretical studies[4] predict that the thermal resistance of a grain boundary approaches a constant value for $T > \theta_D/2$, where θ_D is the

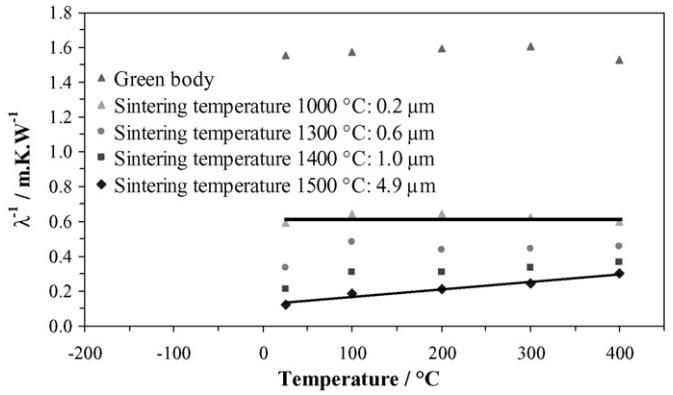

Fig. 4. Thermal resistivity of a green body in temperature compared with the samples sintered above 1000 °C—sintering temperature and grain size are also indicated.

Debye temperature. In contrast the large grain sample (4.9 μm) yields a steady linear increase with temperature corresponding to phonon–phonon scattering and therefore predominance of the intrinsic thermal conductivity of the grains. The transition from one type of behaviour to the other has been qualitatively simulated with Eqs. (3) and (4).

It could be assumed as a first approximation that the grain size variation between the tin oxide green body and the sample fired at 1000 °C is small. The much higher value of thermal resistivity (factor of 2.5) compared to the sintered sample for the green body can then be explained by a much smaller contact area between the grains in the pressed powder compact. This is consistent with the microscopic numerical models. We note also that λ^{-1} does not vary significantly with temperature.

Finally, very similar behaviour was obtained for a green body of alumina. The thermal conductivity at room temperature was 0.6 W m^{-1} K^{-1} with little variation as a function of temperature up to 400 °C. If reduced contact area at the grain–grain interfaces is not taken into account, Eqs. (3) and (4) can be used to predict a value of $\lambda = 6.5$ W m^{-1} K^{-1} using $\upsilon_p = 0.40$, an average grain size of 0.3 μm and $\lambda_{crystal} = 35$ W m^{-1} K^{-1}. This calculation, and the relative similarity of experimental thermal conductivity values between tin oxide and alumina, imply an important role of the contact area of grain–grain interfaces in the thermal conductivity of a green body.

5. Conclusions

This study has examined the effects of the nature of the grain–grain contact and grain growth on the thermal conductivity of a porous polycrystalline oxide originating from a pressed powder compact.

During the sintering step, the formation of grain boundaries and the increase of the contact area between the grains strongly increase the thermal conductivity of the material. Values and behaviour in temperature of thermal conductivity for green bodies of alumina and tin oxide are very similar. The lack of significant variation as a function of temperature suggests that grain–grain interface resistances with very small contact area predominantly control the thermal conductivity of a green body. This conclusion is consistent with numerical simulation of situations at the microscopic scale where the interface resistance and contact area have been used as variables for study.

We have also shown for porous consolidated samples that with the increase of the average grain size the intrinsic thermal conductivity of the grains becomes increasingly significant compared to the thermal resistance of the grain boundaries. In this case the thermal resistivity behaviour in temperature passes gradually from a constant value to a steady linear increase.

In the near future we plan to study variation of contact area in numerical simulation of the geometry in the Coble model and to extend the approach to other ceramic materials with different values of intrinsic thermal conductivity.

Acknowledgements

Céline Poulier would like to express her gratitude towards the Limousin Region and the European Social Fund for financial support of the present work.

References

1. Coble, R. L., Effects of particle-size distribution in initial-stage sintering. *J. Am. Ceram. Soc.*, 1973, **56**(9), 461–466.
2. Smith, D. S., Grandjean, S., Absi, J., Kadiebu, S. and Fayette, S., Grain-boundary thermal resistance in polycrystalline oxides: alumina, tin oxide, and magnesia. *High Temp. High Press.*, 2003/2004, **35/36**, 93–99.
3. Landauer, R., The electrical resistance of binary metallic mixtures. *J. Appl. Phys.*, 1952, **21**(7), 779–784.
4. Young, A. and Maris, H. J., Lattice-dynamical calculation of the Kapitza resistance between fcc lattices. *Phys. Rev. B*, 1989, **40**(6), 3685–3693.